SCIENCE CHINA
Chemistry

• REVIEWS •
• SPECIAL TOPIC • Biophysical Chemistry

December 2014 Vol.57 No.12: 1646–1661
doi: 10.1007/s11426-014-5233-5

Advanced experimental methods toward understanding biophysicochemical interactions of interfacial biomolecules by using sum frequency generation vibrational spectroscopy

YE ShuJi[1,2*] & LUO Yi[1,2]

[1]*Hefei National Laboratory for Physical Sciences at the Microscale and Department of Chemical Physics, University of Science and Technology of China, Hefei 230026, China*
[2]*Synergetic Innovation Center of Quantum Information & Quantum Physics, University of Science and Technology of China, Hefei 230026, China*

Received July 9, 2014; accepted August 6, 2014; published online November 3, 2014

Sum frequency generation vibrational spectroscopy (SFG-VS) has been demonstrated to be a powerful technique to study the interfacial structures and interactions of biomolecules at the molecular level. Yet most previous studies mainly collected the SFG spectra in the frequency range of 1500–4000 cm^{-1}, which is not always sufficient to describe the detailed interactions at surface and interface. Thorough knowledge of the complex biophysicochemical interactions between biomolecules and surface requires new ideas and advanced experimental methods for collecting SFG vibrational spectra. We introduced some advanced methods recently exploited by our group and others, including (1) detection of vibration modes in the fingerprint region; (2) combination of chiral and achiral polarization measurements; (3) SFG coupled with surface plasmon polaritons (SPPs); (4) imaging and microscopy approaches; and (5) ultrafast time-resolved SFG measurements. The technique that we integrated with these advanced methods may help to give a detailed and high-spatial-resolution 3D picture of interfacial biomolecules.

protein, cholesterol, 3D interfacial structures, fingerprint region, amide III, chiral polarization, surface plasmon polaritons, time-resolved

1 Introduction

The interface between biomolecules (e.g., amino acids, lipid, peptides, proteins, DNA, RNA, antibodies) and a surface is one of the most ubiquitous environments on earth and in the human body. One important example of such an interface is biological membranes, which are vital components that constitute the barrier between the inside and the outside of a living cell [1]. The interactions between biomolecules and natural surfaces are essential to human well-being. These interactions are not only critical for many cellular processes such as ion transport and cell signaling in a controlled manner [2, 3], but also play a crucial role in many technological processes including bioseparation, biosensing, biofouling, biomedical implants, and medicine/drug delivery [4–6]. Aside from the natural surfaces that already exist, a number of new artificial surfaces are being developed by combination of science and technology. The rapid growth in nanotechnology greatly enhances the probability of interaction among engineered nanomaterials, humans and the environment, which may result in a series of nanoparticle/biological interfaces [7]. These interactions between nanoparticles and biomolecules (proteins, membranes, cells, DNA, and organelles) lead to the formation of particle wrapping, protein coronas, intracellular uptake and bio-catalytic processes that are directly related to biocompatibility and biodiversity [7]. It is urgent for the emerging

*Corresponding author (email: shujiye@ustc.edu.cn)

discipline of bio-interface science to achieve a better understanding of the interactions between biomolecules and surfaces. However, such interactions are still poorly understood due to their complexity as well as the lack of surface-sensitive and label-free techniques. Consequently, solutions to many scientific problems associated with the characterization of such interactions and biomolecular structures at the interface remain elusive. For instance, conceptual structural models for cholesterol-lipid interactions have been the subject of a long lasting debate even though it is well known that the organization and transport of the cholesterol within cell membrane are critical for human health and many cellular functions [8–10]. Furthermore, accurate determination of protein structures and dynamics at interface [11] and knowledge of interactions at the nano-bio interface are two of the most challenging areas within biology and chemistry today [7].

Addressing the complex interactions at bio-interfaces demands new ideas and *in situ*, real-time and label-free surface methodologies. Techniques such as spectroscopic methods including nuclear magnetic resonance (NMR) and X-ray diffraction have been used to probe the structures of bulk biomolecules. However, most of the current bioanalytical methods that are used to characterize bulk molecules are not sensitive enough to map the inherently small number of molecules bound to a surface. Techniques such as X-ray photo-electron spectroscopy (XPS), secondary ion mass spectrometry (SIMS), scanning electron microscopy (SEM), and scanning tunneling microscopy (STM) are powerful surface-sensitive analytical tools [12], but they require high vacuum to operate or suffer from interference from the surrounding environment, or need exogenous labels. Therefore, they are difficult to be applied to the study of liquid surfaces/interfaces or buried solid interfaces where most interfacial biomolecules are located. In contrast to the methods mentioned above, sum frequency generation vibrational spectroscopy (SFG-VS) has been demonstrated to be a label-free and highly surface-sensitive method that allows study of molecular structures at interface in different conditions [13–17]. It has several advantages over other analytical techniques: it is intrinsically surface-sensitive, requires small amounts of samples, and can probe surfaces and interfaces *in situ* in real time [18]. SFG-VS has been applied to the structure and orientation of various molecules in interfacial environments [4, 11, 13–18] in studies that have been summarized in more than 250 review papers. Yet most of these studies have focused on collecting the spectra in the frequency range of 1500–4000 cm^{-1}.

As mentioned above, the interactions between biomolecules and surfaces are very complicated. The biomolecules themselves are also complex. For example, the membrane of a biological cell is actually a diverse system that is composed of lipids, proteins, carbohydrates and other molecules such as cholesterol [1, 2]. Because all of the compositions are made up of the elements of C, H, O, and N, different molecules may have similar functional groups. Accordingly, only measuring SFG vibrational spectra in the frequency range of 1500–4000 cm^{-1} may not be enough to unambiguously differentiate interfacial biomolecules' structures and interactions. New ideas and advanced experimental methods are therefore indispensable to get more information from the SFG vibrational spectra. In this paper, we introduce some advanced experimental methods for collecting SFG vibrational spectra that our group and others have recently developed. These methods include: (1) detection of vibration modes in the fingerprint region; (2) combination of chiral and achiral polarization measurements; (3) SFG coupled with surface plasmon polaritons (SPPs); (4) imaging and microscopy approaches; and (5) ultrafast time-resolved SFG measurement. It is evident that these advanced methods can determine structures more accurately and give a clearer picture of the interactions of biomolecules at surfaces or interfaces.

2 Brief introduction of SFG-VS

SFG-VS is a second-order polarized nonlinear laser technique that involves two pulsed polarized laser beams that are overlapped spatially and temporally on the sample surface (Figure 1). One is a pulsed visible beam (with a fixed frequency in the visible frequency range (ω_{Vis})) and the other is an infrared beam (with a tunable or broad-band frequency in the infrared frequency range (ω_{IR})). These two overlapped input beams generate a coherent SFG signal at the sum frequency of the two input beams ($\omega_{SFG} = \omega_{IR} + \omega_{Vis}$). As described elsewhere [13–17], under dipolar approximation, bulk materials that possess inversion symmetry do not generate a sum frequency signal; however, surfaces and interfaces where the symmetry is broken do generate a sum frequency signal. The intensity of the SFG light is linear to the intensity of the two input fields $I_1(\omega_{Vis})$ and $I_2(\omega_{IR})$ and the square of the sample's second-order nonlinear susceptibility ($\chi^{(2)}_{eff}$), as shown in Eq. (1).

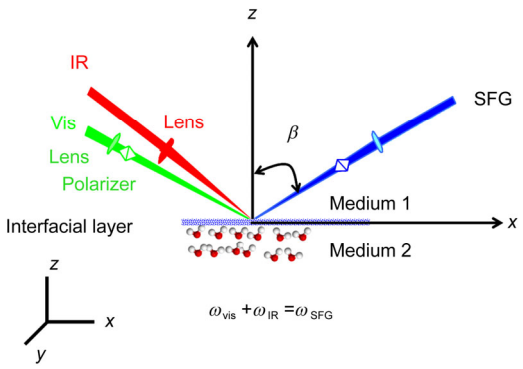

Figure 1 Schematics of SFG experimental geometry.

$$I(\omega_{\mathrm{SFG}}) = \frac{8\pi^3 {\omega_{\mathrm{SFG}}}^2 \sec^2\beta}{c^3 n_1(\omega_{\mathrm{SFG}}) n_1(\omega_{\mathrm{Vis}}) n_1(\omega_{\mathrm{IR}})} \times \left|\chi^{(2)}_{\mathrm{eff}}\right|^2 I_1(\omega_{\mathrm{Vis}}) I_2(\omega_{\mathrm{IR}}) \quad (1)$$

where c is the speed of light; $n_i(\omega_j)$ is the refractive index of medium i at frequency ω_j; β is the incident angle of the SFG beam (Figure 1); and $\chi^{(2)}_{\mathrm{eff}}$ is the effective nonlinear susceptibility corrected by the respective Fresnel factors.

As the IR beam frequency is tuned over the vibrational resonance of interfacial molecules, the effective surface nonlinear susceptibility $\chi^{(2)}_{\mathrm{R},ijk}$ is enhanced. The subindices ijk are the Cartesian coordinates x, y, and z. The frequency dependence of $\chi^{(2)}_{\mathrm{eff}}$ is described by Eq. (2).

$$\chi^{(2)}_{\mathrm{eff}}(\omega) = \chi^{(2)}_{\mathrm{NR}} + \chi^{(2)}_{\mathrm{R},ijk} = \chi^{(2)}_{\mathrm{NR}} + \sum_{\upsilon} \frac{A_\upsilon}{\omega - \omega_\upsilon + i\Gamma_\upsilon} \quad (2)$$

where A_υ, ω_υ, and Γ_υ are the strength, resonant frequency, and damping coefficient of the vibrational mode (υ), respectively. A_υ could be either positive or negative, depending on the phase of the vibrational mode. A plot of SFG signal versus IR input frequency shows a polarized vibrational spectrum of the interfacial molecules. A_υ, ω_υ, and Γ_υ can be extracted by fitting the spectrum.

In terms of polarization of the electromagnetic wave of a polarized light, the light is split into p and s polarizations. The polarized component that is parallel to the plane of incidence is called p polarization, and the component that is polarized perpendicularly to the plane of incidence is called s polarization. Under the SFG experimental geometry shown in Figure 1, the p-polarized light may be resolved into surface electric fields at both the x axis and z axis at the surface, whereas the s-polarized light has a component solely in the y direction [13–17]. Because the SFG light, visible, and IR beams all can be p or s polarization, there are 8 polarization combinations, resulting in 27 elements of $\chi^{(2)}_{ijk}$ (Table 1).

Table 1 Polarization combinations and the elements of $\chi^{(2)}_{ijk}$ that contribute to the SFG spectra

Polarization combinations [a]	Elements of $\chi^{(2)}_{ijk}$
SSP	$\chi^{(2)}_{yyz}$, $\chi^{(2)}_{yyx}$
SPS	$\chi^{(2)}_{yzy}$, $\chi^{(2)}_{yxy}$
PPP	$\chi^{(2)}_{xxx}$, $\chi^{(2)}_{zzz}$, $\chi^{(2)}_{xxz}$, $\chi^{(2)}_{zxx}$, $\chi^{(2)}_{xzx}$, $\chi^{(2)}_{zxz}$, $\chi^{(2)}_{zzx}$, $\chi^{(2)}_{xzz}$
PSS	$\chi^{(2)}_{zyy}$, $\chi^{(2)}_{xyy}$
PSP	$\chi^{(2)}_{xyx}$, $\chi^{(2)}_{xyz}$, $\chi^{(2)}_{zyx}$, $\chi^{(2)}_{zyz}$
SPP	$\chi^{(2)}_{yzz}$, $\chi^{(2)}_{yzx}$, $\chi^{(2)}_{yxz}$, $\chi^{(2)}_{yxx}$
PPS	$\chi^{(2)}_{zzy}$, $\chi^{(2)}_{zxy}$, $\chi^{(2)}_{xzy}$, $\chi^{(2)}_{xxy}$
SSS	$\chi^{(2)}_{yyy}$

a) The polarizations are given in this order: SFG output, visible input, infrared input.

3 Overall view of SFG-VS application on interfacial biomolecules

Since the first SFG study was reported by Shen *et al*. [19, 20] in 1987, SFG-VS has been used by many research groups to investigate molecular structures and interactions at surfaces and interfaces. SFG-VS has also been applied to study the molecular structures and interactions of various biomolecules at surfaces and interfaces. Overall, in terms of biomolecules, the applications include lipid [21–32], vesicle [33], cell [34–37], cellulose [38, 39], starch [40], cholesterol [41–45], amino acids [46–48], peptide and protein [11, 18, 49–56], lipase [57, 58], and DNA [59, 60]. In terms of scientific questions, the applications include bacterial adhesion [61], peptide absorption [62, 63], peptide immobilization [64–66], lipid-membrane interaction [11, 18, 49–56], ligand-protein recognition [67], lipase activity [57, 58], ion-channel formation [68], ionic effects on biointerfaces [69, 70], hydrophobic mismatching [71, 72], nanomaterials and lipid interactions [73], lipid phase kinetics [29], and lipid flip-flop [74]. Numerous reviews have summarized these applications [51–55, 75–88]. For example, Hore *et al*. [51] recently published an excellent review paper to introduce the study on biomolecular structure at solid-liquid interfaces using SFG-VS. We wrote a book chapter to introduce how to use SFG-VS to determine the structure and orientation of interfacial proteins [52]. Table 2 contained a list of the review papers published since 1994 [51–55, 75–88]. Summarily, SFG vibrational spectra can provide the following information about surfaces and interfaces: (1) the kinds of molecular species (or chemical groups); (2) the ordered or disordered degree of the molecules; (3) change in molecular structure; (4) molecular absorption and the orientation of functional groups; (5) interfacial hydrogen-bond networks; (6) assignment of vibrational modes; and (7) surface chirality.

4 Advanced experimental methods for SFG study

It is not easy to understand the biophysicochemical interactions of interfacial biomolecules. It requires employing new ideas and developing advanced experimental methods to accurately determine the interfacial molecular structures and dynamics. According to recent SFG-VS studies, the advanced experimental methods mentioned in the introduction section have greatly expanded the possibility of obtaining a

Table 2 Review papers on the SFG-VS applications for biomolecules at surfaces and interfaces [51–55, 75–88]

Year	Title	Biomolecules	Interface	Signals	Ref.
2014	Biomolecular structure at solid-liquid interfaces as revealed by nonlinear optical spectroscopy	Amino acids, peptides and proteins, carbohydrates, DNA, lipids, cells	Solid/liquid	OH, CH_2, CH_3, amide I, N–H	[51]
2014	Sum frequency generation vibrational spectroscopy: a sensitive technique for the study of biological molecules at interfaces	Peptides, proteins, lipid bilayer, nucleic acids	Solid/liquid	CH_2, CH_3, amide I, N–H	[75]
2013	Elucidation of molecular structures at buried polymer interfaces and biological interfaces using sum frequency generation vibrational spectroscopy	polymer materials, protein, model cell membranes, DNA	Air/liquid, air/solid, solid/liquid	OH, CH_2, CH_3, OCH_3, amide I	[76]
2013	Sum-frequency vibrational spectroscopic studies of Langmuir monolayers	Lipid monolayer, membrane-bound water	Air/water	OH, CH_2, CH_3, OD, CD_2, CD_3, PO_2^-	[77]
2013	Structure and orientation of interfacial proteins determined by sum frequency generation vibrational spectroscopy: method and application	Peptides, proteins	Solid/liquid, air/liquid	Amide I	[52]
2013	Characterization of crystalline cellulose in biomass: basic principles, applications, and limitations of XRD, NMR, IR, Raman, and SFG	Cellulose	Air/solid	OH, CH_2, CH_3, OD, amide I	[78]
2013	Nano-bio interfaces probed by advanced optical spectroscopy: from model system studies to optical biosensors	Peptides and proteins, nano-bio interface	Solid/liquid Air/solid	CH_2, CH_3, amide I	[79]
2012	Molecular interactions of proteins and peptides at interfaces studied by sum frequency generation vibrational spectroscopy	Proteins, peptides	Solid/liquid	CH_2, CH_3, CD_2, CD_3, amide I	[53]
2012	Molecular structures of buried polymer interfaces and biological interfaces detected by sum frequency generation vibrational spectroscopy.	Polymers, peptides	Solid/liquid	OH, CH_2, CH_3, $SiCH_3$, amide I	[80]
2011	Chiral vibrational structures of proteins at interfaces probed by sum frequency generation spectroscopy	Peptides and proteins	Air/liquid	CH_2, CH_3, amide I, N–H	[54]
2011	Nonlinear spectroscopy of bio-interface	Polysugars, proteins, biopolymer, SDS surfactant	Air/solid, metal surface,	CH_2, CH_3, OSO_3^{2-}, fingerprint modes	[81]
2009	*In situ* molecular level studies on membrane related peptides and proteins in real time using sum frequency generation vibrational spectroscopy	Lipids, peptides, proteins	Solid/liquid, air/liquid	CH_2, CH_3, CD_2, CD_3, amide I	[55]
2009	Nonlinear optical spectroscopy of soft matter interfaces	Phospholipid monolayer, colloidal surface	Air/water Solid/liquid, air/solid	CH_2, CH_3	[82]
2009	Optical methods for the study of dynamics in biological membrane models	Lipid monolayer	Air/liquid	OH, CH_2, CH_3	[83]
2009	Sum frequency generation studies on bioadhesion: elucidating the molecular structure of proteins at interfaces	Fibrinogen, factor XII, mefp-3	Solid/liquid	CH_2, CH_3, amide I,	[84]
2006	New insights into lung surfactant monolayers using vibrational sum frequency generation spectroscopy	Lipid monolayer, surfactant monolayer	Air/water	CH_2, CH_3, CD_2, CD_3, PO_2^-	[85]
2006	SFG studies on interactions between antimicrobial peptides and supported lipid bilayers	Antimicrobial peptides, lipid bilayer	Solid/liquid	OH, CH_2, CH_3, CD_2, CD_3, amide I	[86]
2005	Sum frequency generation vibrational spectroscopy studies on molecular conformation and orientation of biological molecules at interfaces	Proteins, peptides, amino acids, lipid monolayers, lipid bilayers,	Solid/liquid, air/liquid	CH_2, CH_3, amide I, amide A,	[87]
1996	What do nonlinear optical techniques have to offer the biosciences?	Amine monolayer, lipid	Air/water	OH, CH_2, CH_3	[88]

thorough knowledge of interfacial biomolecules. Our discussion here begins with the SFG studies on the detection of fingerprint-region vibrational modes.

4.1 Detection of vibrational modes in fingerprint region

Molecular vibrational spectra have been proven to be a highly sensitive way to probe molecular structures and interactions [89, 90]. The vibrational frequencies are split into two regions: functional-group region (4000–1500 cm^{-1}) and fingerprint region (1500–400 cm^{-1}) [22, 91]. The vibrational peaks in the functional-group region are characteristic of specific kinds of bonds. But the molecules with the same functional groups have similar spectra. The peaks in the fingerprint region are contributed by the skeletal vibrations of the molecule or some particular bond stretching (C–O [92], CF_2/CF_3 [93], surfactant sulphate group [94–96], phospholipid phosphate group [22], carboxylate [93], azo group [97], and flavin aromatic ring [98]). In general, the bands associated with skeletal vibrations are likely to conform to a unique fingerprint of the entire molecule or large fragments of the molecule, rather than a specific group within the molecule [91]. In short, the functional group

region can be used to identify which kind of functional group is present, whereas the fingerprint region can be used to positively identify the molecule when its information is used with information indicated by the functional-group region.

As shown in Table 2, SFG-VS is extensively utilized to probe the vibrational modes in the functional group region, yet studies in the fingerprint region are quite rare because of the limited tunability of IR light sources [51–55, 75–88]. With the recent and continuing development of more powerful and reliable pulsed-infrared laser sources (picosecond and femtosecond), it has become possible to detect the vibrational modes in the fingerprint region. Currently, the studies of interfacial biomolecules in the fingerprint region can be classified into three main subjects: head-group motions of surfactant or phospholipid molecules, skeletal vibrations of biopolymers, and amide III signals of proteins.

Head group motions of the surfactant and phospholipid molecules

Amphipathic molecules such as phospholipid are important components of cell membranes. These molecules consist of hydrophobic tailed alkyl chains and hydrophilic head groups. Although the tailed alkyl chains have been well studied by probing the CH_2 and CH_3 functional groups, few reports have been submitted on the head groups whose vibrational frequencies are typically in the fingerprint region. Richmond *et al*. [95, 96] reported the first SFG measurement of the molecular structure and orientation of the head group of a charged alkyl surfactant. They used sodium dodecyl sulfate (SDS) as a prototype system and demonstrated how to use polarization experiments to determine the interfacial orientation of sulfate modes (SO_3 symmetric stretch) in the 1100 cm^{-1} region [95, 96]. Subsequently, the Allen group studied the hydration behavior of the phosphate group of a DPPC lipid monolayer by measuring the frequency in the fingerprint region [22]. They observed the peak position of the PO_2^- symmetric stretch in the liquid-expanded (LE) phase at about 1094 cm^{-1} and that it shifted to higher frequency at 1104 cm^{-1} upon compression to the liquid-condensed (LC) phase (Figure 2). They were able to well explain the change in hydration state of the DPPC monolayer using a water-squeeze-out process model because the strong hydrogen-bonding network between water molecules and the phosphate group in the LE phase weakened the PO_2^- bonds and then led to peak-shift at a lower frequency (1094 cm^{-1}) than the LC phase (1104 cm^{-1}). They finally concluded that lipid head-group hydration is a crucial factor regulating lung-surfactant interfacial behavior during inhalation and exhalation [22].

The skeletal vibrations of biopolymers

In principle, the structure and orientation of a small molecule can be determined by detecting its functional groups. However, biomolecules such as polymers, peptides, and proteins are usually very large and have quite complicated structures. They can form structures at different-level (i.e., primary, secondary, and tertiary). Because the different-level structures have the same functional groups, it is impossible to access the details of secondary and tertiary structures by analyzing the functional groups alone. By contrast, the skeletal vibrations in the fingerprint region often arise from the movement of several chemical groups

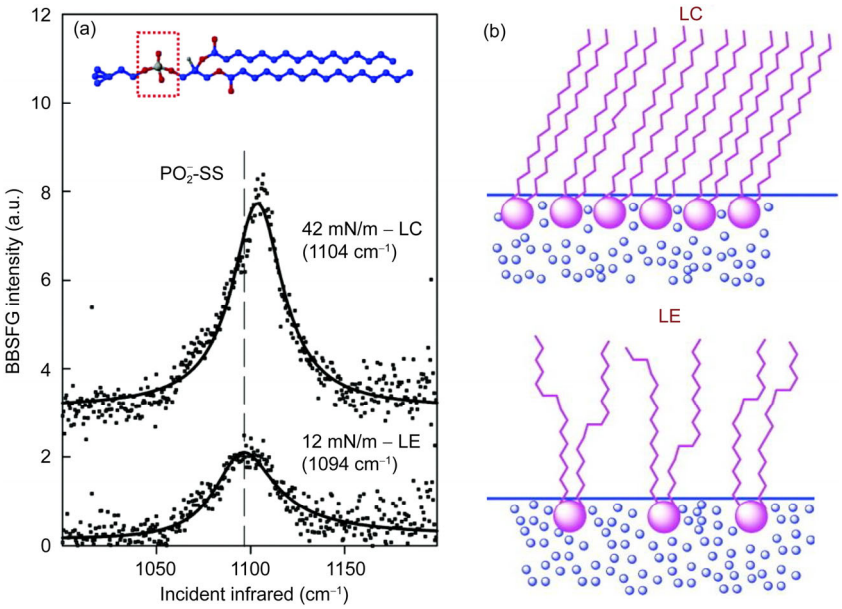

Figure 2 (a) SSP BBSFG spectra of the DPPC-d_{62} monolayer in the fingerprint region at two different surface pressures; (b) illustration of the water-squeeze-out process (blue dots representing water molecules) [22].

or an entire molecule, rather than a localized vibration of single chemical bond. These delocalized modes are extremely sensitive to the backbone conformation and tertiary 3D structure changes in a molecule. Therefore, it is feasible to deduce complicated 3D structures by probing the vibrational modes in the fingerprint region combined with the modes in functional group region. In order to get high-power pulsed-infrared energy for SFG experiments in the fingerprint region, Roke *et al*. [99] developed a modified Ti:Sapphire laser based on a three-stage chirped-pulse amplification scheme. Using the pulses from that system, they measured the fingerprint-region delocalized modes of a biopolymer (poly(lactic acid) (PLA)) with different crystalline states and successfully determined its 3D surface structure as amorphous L-PLA (L-A), crystalline L-PLA (L-C), and racemic D/L-PLA (R) (Figure 3) [100]. By probing the delocalized vibrational modes, they observed dramatic changes in the 3D arrangement of the surface molecular backbones (Figure 3(a)). This type of information could not be obtained from probing only localized group modes (Figure 3(b)).

Amide III signal of proteins and peptides

Proteins (peptides) are essential for humans and are especially important molecules of cell membranes. The studies on interfacial structures of proteins and peptides at interfaces are extremely important because they can provide vital understanding in many important fundamental research projects and real applications. It has recently been demonstrated that SFG-VS is a unique and powerful technique for probing structures of peptides and proteins at interfaces. The backbone vibrations of proteins are known as the amide vibrations in three different energy regions, known as amide I, II, and III. Because the signals of amide II and amide III bands are too feeble to be detected, previous research has mainly focused on the side-chain signals and amide I signals in SFG-VS studies. It is evident that α-helical and β-sheet structures can be identified by probing the backbone amide I vibration. However, the amide I vibrations (which arise mainly from the C=O stretching vibration with minor contributions from the out-of-phase C–N stretching vibration) have at least three weaknesses. The first weakness is that the amide I signals are seriously overlapped with the signal from water bending modes at ~1645 cm^{-1}. Therefore, infrared (IR) energy loss due to the absorption in atmosphere by water vapor can often introduce some errors and uncertainties in interpretation of SFG-VS results. The second weakness is that the characteristic amide I bands of various secondary structures are clustered in the spectral region of 1600–1700 cm^{-1}. The third weakness is that the center frequency of α-helical and random-coil structures overlap in the frequency of ~1655 cm^{-1} [101, 102]. Consequently, it becomes extremely difficult, if not impossible, to accurately differentiate the random-coil and α-helical structures at the interface. Conversely, the so-called amide III_3 bands (denoted as amide III below) comprise the spectral range between about 1200 and 1400 cm^{-1} and no water interference occurs in this region [103]. Amide III bands are predominated by the in-phase combination of C–N stretching and N–H in-plane bending. For various secondary structures of proteins, amide III bands are more resolved and better defined than amide I bands. Because the amide III frequency is known to be particularly sensitive to the polypeptide backbone conformation and tertiary structure, consideration of the amide III bands can, at least in principle, resolve the difficulties in determining interfacial protein structures using amide I bands. Accordingly, it is important

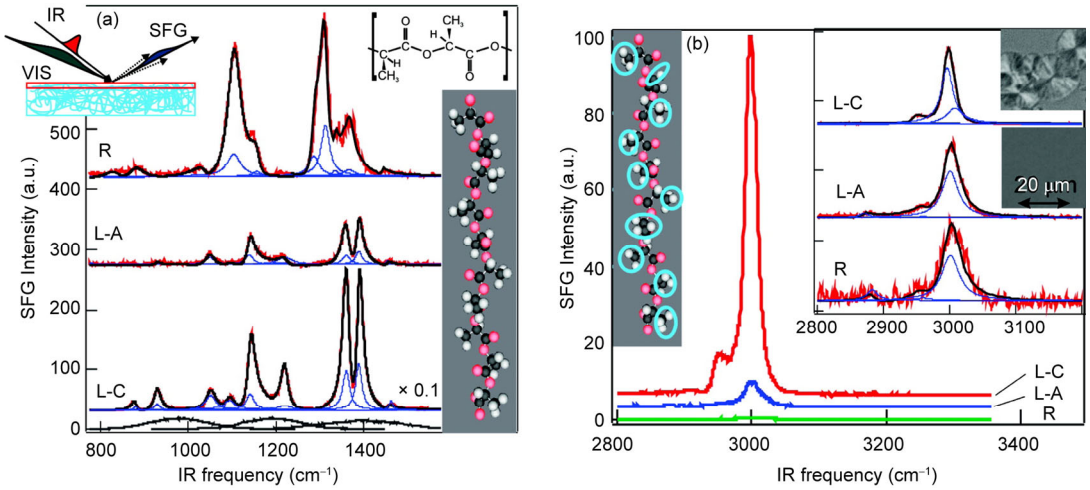

Figure 3 (a) SFG spectra of L-crystalline (L-C), L-amorphous (L-A), and racemic (R) PLA films in the fingerprint region (taken with three different IR pulses, which are displayed at the bottom); (b) SFG spectra of the same structures in the functional-group region. The right insert of (b) shows the Crossed-polarized microscopy images of the L-C and L-A films which reflect the difference in the state of the films. SFG-VS experimental geometry and Chemical repeat unit of L-PLA are illustrated in the left insert of (a) [100].

to extend SFG-VS studies to the fingerprint region to get more useful information with which to elucidate the molecular structure of peptides and proteins at interfaces. Certainly, it is impossible to determine interfacial protein structure using amide III bands alone. To address this measurement gap in the structural characterization of interfacial proteins, we recently demonstrated for the first time that SFG-VS can unambiguously differentiate interfacial protein secondary structures by combining surface-sensitive amide I and amide III spectral signals [11]. In order to obtain the hardly-measureable SFG signals in the amide III region, we recently employed several newly developed technical procedures: (1) a near-total-internal-reflection geometry; (2) assigning higher voltage to the detector of PMT; and (3) equipping a new and longer difference-frequency generation (DFG) crystal to generate a stable IR pulse with energy > 20 μJ. With these improvements, we have successfully probed the very weak amide III signals of several antimicrobial peptides (AMPs) in negatively charged lipid bilayers (Figure 4) [11]. These AMPs include LKα14, mastoparan X (MP-X), cecropin P1 (CP-1), pardaxin, and melittin. Although NMR and CD results suggested that these peptides have different helicities [11], the SSP spectra in the amide I region (Figure 4(B)) are all dominated by a single resonance peak centered at 1655 cm^{-1}, which does not permit us to distinguish the random-coil structure from the α-helical structure. In contrast to a single peak observed in the amide I region, the amide III spectra (Figure 4(C)) show two peaks with the frequencies below (Peak 1, Figure 4(C-e)) and above (Peak 2, Figure 4(C-a)) 1260 cm^{-1}. A linear correlation is also clearly observed between the peak amplitude ratio of $\chi^{(2)}_{Peak1} / \chi^{(2)}_{Peak2}$ and the content ratio of the disordered structure [11]. As indicated in Figure 4, the method that combines surface-sensitive amide I and amide III spectral signals can unambiguously identify the α-helical and random-coil structures for interfacial proteins, which resolves one of the most important long-standing problems in interfacial protein science [11].

By monitoring an amide III signal, we can also get an in-depth insight into how the lipid-charge status and the solution ions affect the interfacial interaction between peptides and model cell membranes. Figure 5(A) shows the SSP amide III spectra of pardaxin in fully negatively charged DMPG and partly negatively charged DMPC/DMPG (molecular ratio = 3:1) bilayer. The intensity ratio between the peak at ~1230 cm^{-1} (Peak 1) and the peak at ~1280 cm^{-1} (Peak 2) ($\chi^{(2)}_{Peak1} / \chi^{(2)}_{Peak2}$) increased from 0.34 to 0.73 when the negative charge of the membrane decreased from 100% to 25%. This result indicates that pardaxin undergoes a conformational change from the random-coil structure to the α-helical structure with the increase of the fraction of the negatively charged lipids. Figure 5(B) presents the time-dependent spectra in the amide III region after a certain amount of phosphate buffer solution was injected into the melittin-DPPG bilayer system. Following the addition of the salt solution, we observed that the signals of the peaks at ~1230 and ~1280 cm^{-1} both gradually increased, whereas the ~1115 cm^{-1} peak from symmetric mode of PO_2 decreased and finally disappeared. This information deduced from the signals in the amide III region may suggest that the interaction between melittin and DPPG bilayer in the phosphate buffer solution follows a toroidal model. The phosphate ions may also change the helicity of melittin.

4.2 Combination of chiral and achiral polarization measurements

Chiral molecules are the molecules that can not be superimposed by translation and rotation on their mirror images [104, 105]. Accordingly, chiral molecules do not have

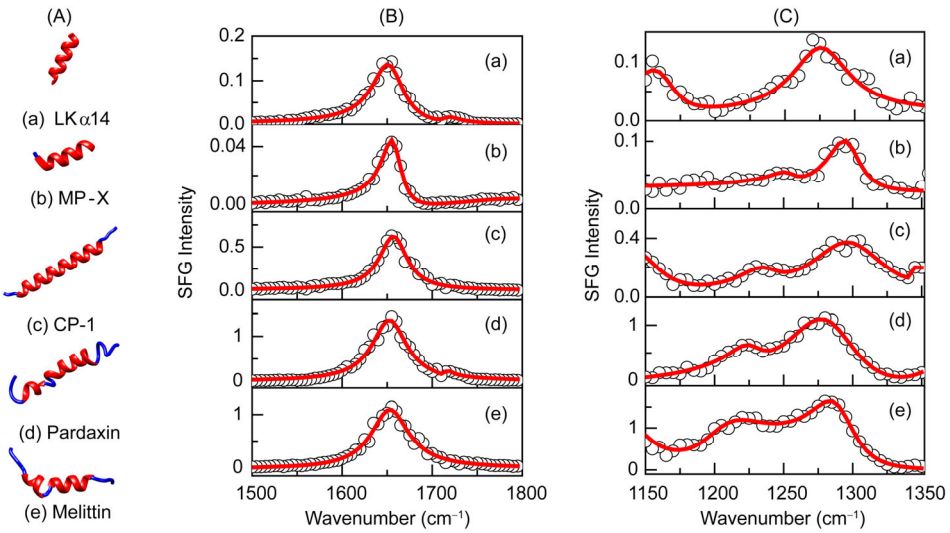

Figure 4 The SSP amide spectra of the peptides in lipid bilayers [11]. (A) Schematics of secondary structures with red helix and blue random coil given by NMR studies; (B) the amide I spectra; (C) the amide III spectra. (a) LKα14; (b) MP-X; (c) CP-1; (d) pardaxin; (e) melittin.

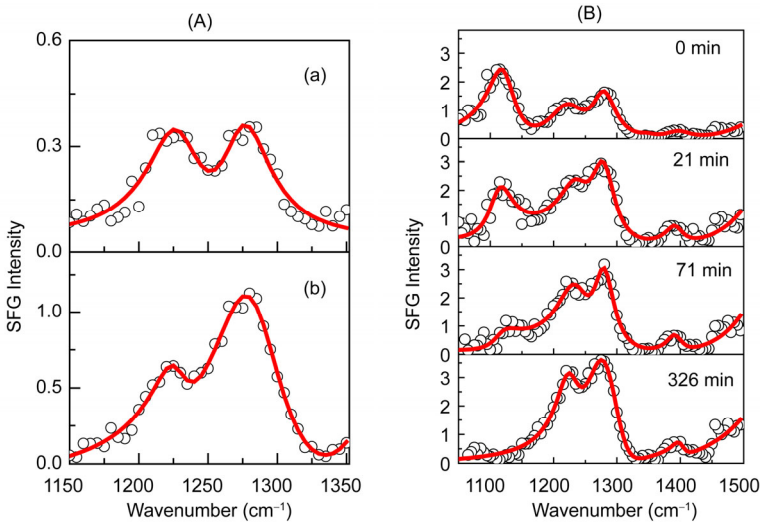

Figure 5 (A) The amide III SSP spectra of pardaxin in mixed DMPC/DMPG (3/1) bilayer (a) and pure d-DMPG lipid bilayer (b); (B) time-dependent spectra in amide III region after a certain amount of phosphate buffer solution was injected into the melittin-DPPG bilayer system [11].

symmetry planes, inversion centers, or improper rotation axes. Because of the lack of inversion symmetry in chiral molecules, SFG is a specifically powerful and effective method for probing molecular chirality [106–108]. In terms of the features of a chiral molecule, the 3D characteristics of chirality require the three subindices *ijk* of $\chi^{(2)}_{\mathrm{R},ijk}$ to be different ($i \neq j \neq k$) [104, 105]. In other words, the polarization combinations of PSP, SPP, and PPS in Table 1 are termed as chiral polarizations while others are achiral polarizations. Thus surface chirality can be probed by using the PSP, SPP, and PPS polarizations. In this case, the interference from the backgrounds of achiral solute and solvent molecules at the interface can be eliminated because the SFG signals from the achiral molecules are all silent in PSP (or SPP or PPS) spectra [104, 105].

In nature, most molecules in natural biological systems are chiral, from amino acids to sugars, nucleic acids, proteins, and hormones [106–110]. For example, except for glycine, all amino acids have a chiral carbon center. Chiral molecules have been considered to be the backbones of all life forms. Therefore, SFG measurements that combine chiral and achiral polarization will be indispensable for the characterization of the molecular structures and interactions of biomolecules at surfaces and interfaces. However, chiral SFG studies are unusual compared to the thousands of SFG reports in web of science. Only biomolecules such as amino acids [47, 111], peptides and proteins [112–121], 6-ketocholestanol [122], and DNA [123, 124] have been examined using chiral SFG-VS.

The study of peptides and proteins

Peptides and proteins may form different secondary structures (e.g., α-helix, 3_{10}-helix, anti-parallel β-sheet, and parallel β-sheet) [52]. The repeat units of these secondary structures have symmetries of $C_{18/5}$, C_{3v}, D_2, and C_2, respectively. As a consequence, β-sheet structures generate chiral signals but the real helical structures do not (Table 3), which allows us to distinguish the β-sheet structures from the helical structures. The Chen group [117] first developed chiral SFG to probe interfacial protein structures using PSP and SPP polarization combinations. They detected chiral amide I signals from a peptide of tachyplesin I, which forms an anti-parallel β-sheet structure on a polystyrene surface. Later, they developed a method for quantifying the orientation of the interfacial β-sheet structure by analyzing both achiral SSP and chiral PSP SFG spectra in the amide I region, as well as combining attenuated total reflectance Fourier transformation infrared spectroscopic measurements (ATR-FTIR) [118]. Recently, Yan's group not only applied the chiral SFG to identify secondary structures of proteins at interfaces through measuring the chiral and achiral signals in amide I and amide A (N–H) regions [119] but also probed the kinetics of conformational changes of amyloid proteins at lipid monolayer surfaces by using an amide I signal [120]. They also monitored the proton exchange rate in interfacial antiparallel β-sheet proteins using chiral signals in the N–H/N–D regions [121] and examined the self-assembly of an amphiphilic peptide (LK7β) into macromolecular chiral structures by using chiral signals from the C–H stretch [113].

It is worth mentioning that the Yan's group claimed that the chiral N–H signal can be used as a vibrational optical marker to distinguish protein secondary structure at interfaces based on the unique spectral features for the observed random coils, α-helices, and β-sheets at interfaces. They claimed that the α-helix structures show chiral N–H stretch signals but are silent in the amide I chiral spectra, while the β-sheet structures show the amide I chiral spectra, but do not have chiral N–H stretch signals [119]. These conclusions

Table 3 Properties of different types of secondary structures of proteins [52]

Secondary structure	Repeating residues	Symmetry	SFG active modes	Peak center (cm^{-1})	Chiral
α-Helix	3.6	$C_{18/5}$	A, E_1	~1655	No
3_{10}-Helix	3	C_{3v}	A, E_1	~1635	No
Anti-parallel β-sheet	4	D_2	B_1	~1685	Yes
			B_2	~1630	Yes
			B_3	~1720	Yes
Parallel β-sheet	2	C_2	A	~1625	Yes
			B	~1670	Yes

contradict not only our recent study of prion protein [125] but also their own results on proton exchange in antiparallel β-sheets at interfaces [121]. Recently, we used a prion protein fragment (PrP118–135) as a model and investigated the influence of the concentration of the protein fragment on interactions between PrP118–135 and a POPG lipid bilayer [125]. We found that the fragment adopted mostly in α-helices at low concentrations. As the PrP118–135 concentration increased, the SSP signals from the peak at 1657 cm^{-1} at the concentration of > 0.03 mg/mL, which is characteristic of an α-helical structure and are much weaker than those at the concentration of ⩽ 0.03 mg/mL. Conversely, the intensity of PSP signals at 1625 and 3300 cm^{-1} increased with the increasing concentration (Figure 6). By analyzing the SFG spectra at different polarization combinations, we can conclude that the molecular number ratio of parallel β-sheet structures on a POPG bilayer increases with prion concentration and reaches 44% at the prion concentration of 0.10 mg/mL. The α-helical structures were oriented close to perpendicular to the surface normal, while the β-sheet structures were oriented parallel to the lipid bilayer. In addition, our results suggested that the chiral N–H stretch signals (the PSP N–H signals) mainly arise from the α-helical structure due to the leakage of SSP and PPP spectra at low PrP concentrations and from the β-sheet structure at high PrP concentrations. Therefore, the chiral N–H signal cannot be used to distinguish protein secondary structures at interfaces.

Organization and transport of cholesterol

Currently, combination of chiral and achiral polarization measurements is mainly applied to the studies on interfacial peptides/proteins. Recently, we reported the first application of chiral SFG-VS on the organization and transport of cholesterol in a model cell membrane [122]. Cholesterol is a ubiquitous component of mammalian plasma membrane. The organization and transport of the cholesterol within cell membranes are known to be critical for human health and many cellular functions [8, 126]. However, a precise molecular description of cholesterol behavior within a membrane remains elusive due to the lack of surface-sensitive and label-free techniques [8–10]. Cholesterol is a molecule that comprises a near-planar tetracyclic-fused chiral steroid ring and a flexible achiral isooctyl hydrocarbon tail. The chiral sterol ring has two sides: one side is flat and smooth with no substituent (α face), and the other is rough with chiral methyl substitutions (β face). Hence, a combination of achiral-sensitive SSP and chiral-sensitive PSP polarization measurements can permit the explicit differentiation of structural change of cholesterol isooctyl tail and methyl substitutions of cholesterol sterol rings. In this case, the

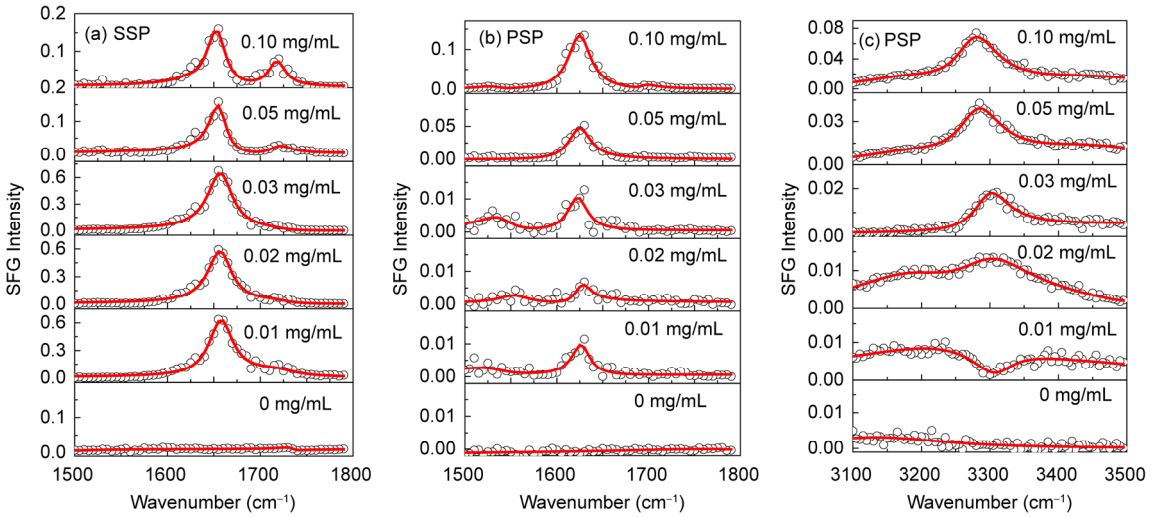

Figure 6 SFG spectra of PrP118–135 in POPG/POPG bilayer at different concentrations in amide I region [125]. (a) SSP in amide I region; (b) PSP in amide I region; (c) PSP in amide A region. Solid line represents the fitting profile.

structural change of chiral methyl substitutions can be monitored using the PSP spectra without interference from lipid, cholesterol hydrocarbon tail, or membrane-bound water molecules. To materialize this idea, we used cholesterol analog 6-ketocholestanol (6-KC) as a model to investigate the interactions between cholesterol and neutral lipid bilayer *in situ* and in real time. 6-KC has a similar structure to cholesterol except with a keto moiety at the position of the B ring (Figure 7(A)) [122]. For such a molecule, there are three possible forms of side-by-side organization on one leaflet: α-α, β-β, and α-β (Figure 7(B)). When a flip-flop of 6-KC occurs, tail-to-tail structure will be organized on both leaflets (Figure 7(C)). This different organization will result in a distinct dependence of SSP and PSP intensities upon the 6-KC concentration. According to the SFG symmetry constraints, the formation of tail-to-tail organization on both leaflets (Figure 7(C)) can effectively cancel the SSP signal. Similarly, the formation of α-α and β-β structures (Figure 7(B-a, b)) can effectively eliminate chiral signal but an α-β structure (Figure 7(B-c)) cannot. We investigated the influence of 6-KC concentration on the SSP and PSP intensities. We observed that the SSP intensity (achiral SFG) follows an almost linear dependence upon the bulk concentration of 6-KC whereas the PSP intensity (chiral SFG) reached a plateau after a certain concentration (Figure 8). Because chiral SFG signals depend mostly on the chiral arrangement of the chiral centers rather than their absolute number, we can conclude that the tail methyl groups of different 6-KC molecules adopt the same orientation direction while the chiral methyl substitutions organize with α-β structure at low 6-KC concentration and α-α or β-β structure at high 6-KC concentration. In addition, we found that the long-anticipated flip-flop motion of the cholesterol does not take place in a lipid bilayer at room temperature. Our results favor the so-called umbrella model with the formation of cholesterol clusters [122].

4.3 SFG coupled with surface plasmon polaritons (SPPs)

High signal-to-noise (S/N) ratio and better spectral resolution are goals that a wide range of scientists continues to pursue. High S/N ratio and better spectral resolution can greatly decrease acquisition times. Because plasmon oscillations in metallic nanostructures can cause large amplification

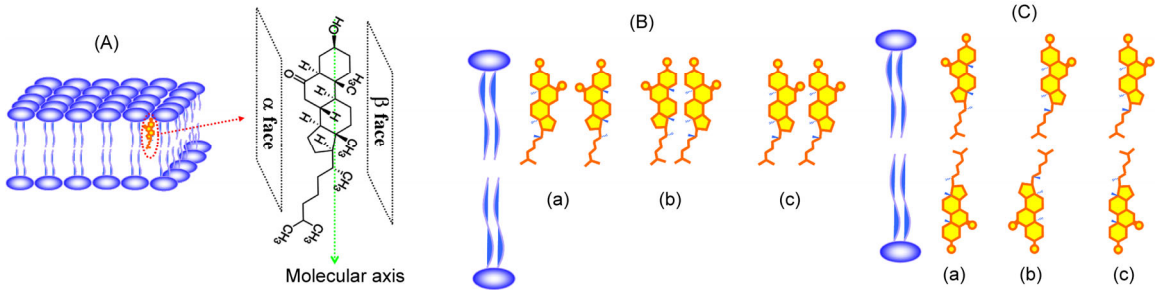

Figure 7 (A) Molecular structure and defined molecular axis of 6-KC; (B) possible forms of side-by-side organization of 6-KC on one leaflet of lipid bilayer ((a) α-α structure; (b) β-β structure; (c) α-β structure); (C) possible forms of 6-KC organizing on both leaflets [122].

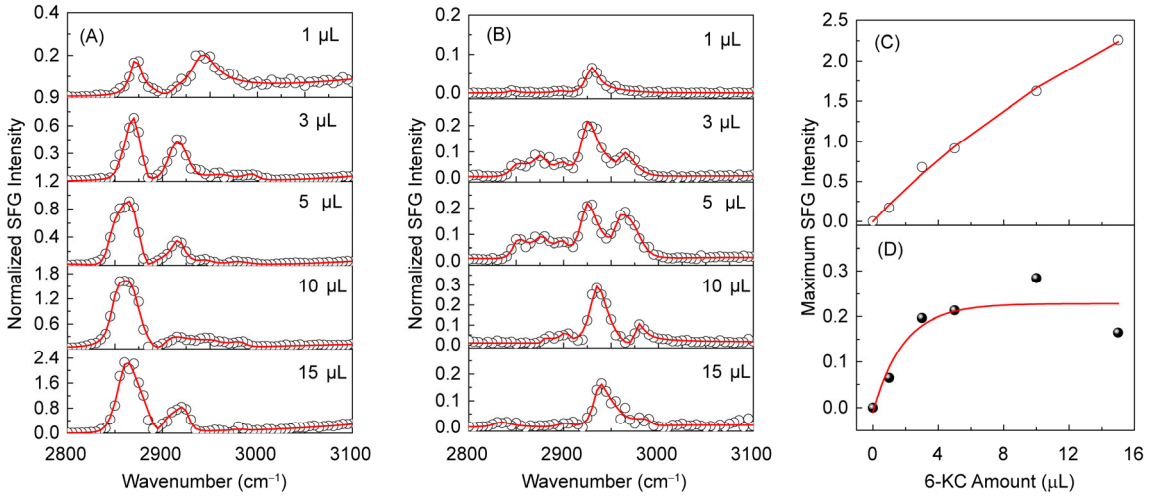

Figure 8 (A) The SSP intensity; (B) PSP intensity change with the 6-KC amount; (C) the maximum SSP intensity at 2865 cm^{-1}; (D) PSP intensity at 2935 cm^{-1} as a function of the 6-KC amount [122].

of the local electric field, surface plasmon polaritons (SPPs) have attracted great attention for their potential applications through spectroscopy [127]. Here, SPPs are electromagnetic waves trapped at the conductor/dielectric interface and evanescently confined in the perpendicular direction [128]. These electromagnetic waves arise via the coupling of the electromagnetic fields to oscillations of the conductor's electron plasma [128]. The coupling of optics with SPPs can largely increase the yield of nonlinear optical processes because the light energy is condensed into subwavelength volumes and can thereby reach higher spectroscopic sensitivity [128–130]. One of the most well- known examples of this effect is surface-enhanced Raman spectroscopy (SERS) [131]. Therefore, coupling of SFG-VS with SPPs may provide a major solution to the problem of accessing high S/N ratio. In fact, SPPs have been proved to be compatible with SFG-VS. To date, several SPPs-enhanced SFG phenomena have been explored. It is evident that the total SFG intensity is enhanced from several tens to ten thousands times. For example, Yakovlev *et al.* [132, 133] first observed that the SFG signals of the thin organic films and fullerene films on silver could be enhanced by excitation of a surface plasmon on silver. Baldelli *et al.* [134] reported that the SFG signal of CO adsorbed on platinum particles of 45 nm diameter was ~10^4 times larger than that from CO on smooth Pt films. Chou *et al.* [135] examined the SFG signals of an octadecanethiol self-assembled monolayer on an AgFON surface and found that the SSP SFG signals were enhanced by up to 730 times. Busson *et al.* [136] showed that an enhancement factor of 21 could be deduced for the SFG signal of thiophenol adsorbed on gold nanoparticles with an average diameter of 17 nm. Lis *et al.* [129] investigated the enhancement of SFG signals from molecules adsorbed on metallic nanopillars excited at a resonance frequency that matched their localized surface plasmons. This nanostructured platform increased the molecular SFG signal of a monolayer by two orders of magnitude (Figure 9) [129]. Most recently, Liu and Shen [137] successfully demonstrated the feasibility of measuring *in situ* and real-time vibrational spectra during electrochemical (EC) reactions at noble metal gold electrodes by using SP-enhanced SFG-VS carried out with Kretschmann geometry (Figure 10). Unfortunately, the application of SFG-VS coupled with SPPs to the research of interfacial biomolecules remains unexplored. Nevertheless, SPPs-enhanced SFG can largely improve spectral sensitivity and specific spatial selectivity, which will make it a promising platform in the development of analytical biomolecular devices.

4.4 Imaging and microscopy approaches

Imaging and microscopy are the best language that physicists, chemists, materials scientists, and biologists can use to communicate with each other easily and directly. Because SFG vibrational imaging and microscopy (SFG-VI, SFG-VM) provide a natural choice to achieve a chemically selective contrast for the interfacial endogenous biomolecules without interference from other off-target molecules, these methods have become important tools for obtaining spatial information about the dynamic process of biological samples, specifically cellular biology at surface and interface [138, 139]. Several groups have modified their SFG-VS systems to SFG-VI (SFG-VM) and have exploited their new systems to study the biomolecules of proteins, lipids and cells. For example, Raghunathan *et al.* [140] developed a rapid vibrational SFG imaging using a tunable picosecond pulse from a high-repetition-rate (76 MHz) optical parametric oscillator and demonstrated that the vibrationally selective imaging of collagen fibers is achieved with submicrometer lateral resolution. Sakai *et al.* [141] used a home-

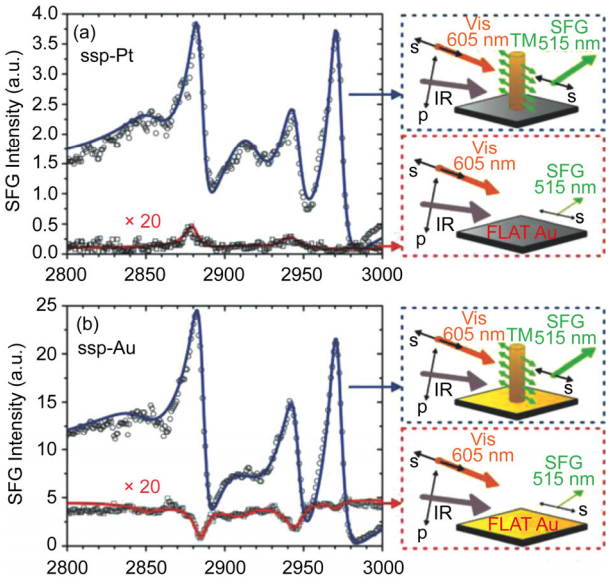

Figure 9 SFG spectra of dodecanethiol molecules chemisorbed on platinum in SSP polarization (a), gold in SSP polarization (b) [129]. Open circles are the SFG intensities from the gold nanopillar zones on the aforementioned surfaces; open squares are the SFG intensities on the bare flat surfaces. The insets sketch the experimental conditions in which the spectra were recorded.

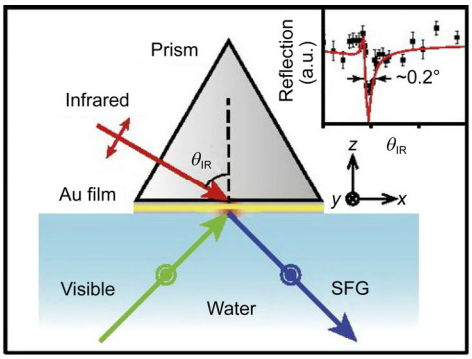

Figure 10 Schematic of an experimental arrangement for an SP-SFVS setup [137].

made SFG-VM with the detected IR wavelength of 6–9 μm to measure the IR super-resolution images of cross sections of a human hair and obtained a submicrometer spatial resolution. Conboy *et al*. [142] built a simplified SFG-VI setup to characterize lipid bilayer arrays asymmetrically prepared by 1,2-distearoyl-sn-glycero-3-phosphocholine (DSPC):1,2-distearoyl (d70)-sn-glycero-3-phosphocholine (DSPC-d70). They successfully exploited this SFG-VI to probe the transition temperature of a patterned DSPC:DSPC-d70 lipid bilayer array and the phase behavior in a multi-component micro-patterned lipid bilayer array (MLBA) prepared using three different binary lipid mixtures (1,2-dioleoyl-sn-glycero-3-phosphocholine (DOPC):DSPC, DOPC:1,2-dipalmitoyl-sn-glycero-3-phosphocholine (DPPC), and 1,2-dimyristoyl-sn-glycero-3-phosphocholine (DMPC):DSPC [142]. Fujii *et al*. [141, 143] used SFG-VI to record the single-cell infrared (IR) imaging of onion (Allium cepa) root cells. As for the applications of SFG-VI and SFG-VM on interfacial biomolecules, in 2013 Chung *et al*. [139] gave a detailed introduction to biomolecular imaging with coherent nonlinear vibrational microscopy. It is worth mentioning that most of the previous SFG microscopy studies collect the SFG signals in the CH-stretching vibrational range and had a limited spatial resolution (up to a few hundred nanometers) due to the diffraction of light or the wavelength of visible light. In order to improve the spatial resolution, a combination of different methods is required. Because the light can be confined to a nanometer region by the excitation of localized surface plasmons at the apex of sharp metal or metal-coated tips [127–131], SPPs-enhanced SFG-VI (SFG-VM) will be feasible to achieve a resolution in tens of nanometers and to improve the S/N ratio for high-speed imaging. In addition, collecting SFG signals in the fingerprint region and using chiral polarization combinations may give a wealth of 3D chemical information [144]. Therefore, the image and microscopy technique integrated with SPPs enhancement, fingerprint region and chiral polarization may help to give a detailed and high-spatial- resolution 3D picture of interfacial molecules.

4.5 Ultrafast time-resolved SFG measurement

Insights into the interfacial molecular structures at static states are necessary but not always sufficient to describe their interaction at surfaces and interfaces. For instance, a complete understanding of the relevant interfacial chemical reactivity and biological processes requires knowledge of interfacial structural dynamics such as the formation of equilibrium surface structures, occurrence of the chemical transformations on surfaces, the coupling between substrate and biomolecules, and the energy transfer or mass transport at the interface, etc. [145–147]. A timescale of these dynamic processes is typically from hundreds femtosecond (fs) to picosecond (ps). Advances in time-resolved SFG-VS experiments may help to provide important information that cannot be obtained from static experiments. In a time-resolved SFG-VS experiment, an intense fs or ps laser pulse in the visible, near-infrared, infrared region is used to pump the sample to cause electronic, vibrational, and thermal excitation of the molecules and substrates. Next, SFG-VS is used to monitor these transient changes in real time at high temporal resolutions to provide direct information about the structural changes induced by the pump-laser pulse [145–147]; these studies are shedding new light on the translational and vibrational dynamics of interfacial molecule [146–151]. For example, Bonn *et al.* [146, 147] used this technique to probe the energy-flow dynamics in model membranes and demonstrated the potential of using time-resolved SFG measurement to elucidate biomolecular dynamics at membrane surfaces. Their studies revealed that an incoherent energy transfer occurs from the excited CH_2 groups to the terminal CH_3 groups in the lipid alkyl chains. It takes less than 1 picosecond for the heat to be transferred from the polar head-group region of the lipid to the end of the alkyl chain. However, applications of these time-resolved SFG experiments are not being widely explored at this time. Instead, studies are mainly focused on small molecules such as water. In addition, although two different kinds of SFG systems, a narrow-band frequency scanning system (FSSFG) [145] or a broad-band IR laser system (BBSFG) [146–151], have been exploited for the time-resolved experiments, only a few groups have constructed time-resolved systems: a near-infrared (1064 nm) pump-FSSFG probe system by the Domen group [145], and an fs UV (visible or infrared beam) pump-BBSFG probe by the Shen [149], Bonn [146–148], Borguet [151], Eisenthal [152], and Tahara groups [153]. Because numerous important biological processes at surface and interface depend on rapid dynamic processes such as fast energy-transfer processes, we believe that time-resolved SFG measurements will play a vital role in the deep understanding of the biophysicochemical interactions of biomolecules at surfaces and interfaces.

5 Conclusions

Herein, we have summarized the advanced experimental methods on collecting SFG vibrational spectra recently developed by our group and others. These methods include: (1) detection of fingerprint-region vibration modes; (2) combination of chiral and achiral polarization measurements; (3) SFG coupled with surface plasmon polaritons; (4) imaging and microscopy approaches; (5) ultrafast time-resolved SFG measurement. It is evident that application of these advanced methods may help to determine structures more accurately and give a clearer picture of the interaction of biomolecules at surfaces or interfaces. Although we focused these methods on interfacial biomolecules, they will be directly feasible for other interfacial molecules as well.

This work was supported by the National Basic Research Program of China (2010CB923300), the National Natural Science Foundation of China (21273217, 91127042, 21161160557), and the Scientific Research Foundation for the Returned Overseas Chinese Scholars, State Education Ministry.

1 Allen JP. *Biophysical Chemistry*. Oxford: Wiley-Blackwell Press, 2008
2 Yeagle PL. *The Structure of Biological Membranes*. Boca Raton, FL: CRC Press, 2005
3 Mateo CR, Gomez J, Villalain J, Gonzalez Ros JM. *Protein-Lipid Interaction: New Approaches and Emerging Concepts*. Berlin: Springer, 2006
4 Castner DG, Ratner BD. Biomedical surface science: foundations to frontiers. *Surf Sci*, 2002, 500: 28–60
5 He LZ, Dexter AF, Middelberg APJ. Biomolecular engineering at interfaces. *Chem Eng Sci*, 2006, 61: 989–1003
6 Garcia AJ. Interfaces to control cell-biomaterial adhesive interactions. *Adv Polym Sci*, 2006, 203: 171–190
7 Nel AE, Madler L, Velegol D, Xia T, Hoek EMV, Somasundaran P, Klaessig F, Castranova V, Thompson M. Understanding biophysicochemical interactions at the nano-bio interface. *Nature Mater*, 2009, 8: 543–557
8 Ali MR, Cheng KH, Huang JY. Assess the nature of cholesterol-lipid interactions through the chemical potential of cholesterol in phosphatidylcholine bilayers. *Proc Natl Acad Sci USA*, 2007, 104: 5372–5377
9 Bennett WFD, MacCallum JL, Hinner MJ, Marrink SJ, Tieleman DP. Molecular view of cholesterol flip-flop and chemical potential in different membrane environments. *J Am Chem Soc*, 2009, 131: 12714–12720
10 Ikonen E. Cellular cholesterol trafficking and compartmentalization. *Nat Rev Mol Cell Biol*, 2008, 9: 125–138
11 Ye SJ, Li HC, Yang WL, Luo Y. Accurate determination of interfacial protein secondary structure by combining interfacial-sensitive amide I and amide III spectral signals. *J Am Chem Soc*, 2014, 136: 1206–1209
12 Brune D, Hellborg R, Whitlow HJ, Hunderi O. *Surface Characterization: A User's Sourcebook*. Wiley-VCH: Scandinavian Science Publisher, 1997
13 Shen YR. *The Principles of Nonlinear Optics*. New York: Wiley, 1984
14 Castellana ET, Cremer PS. Solid supported lipid bilayers: from biophysical studies to sensor design. *Surf Sci Rep*, 2006, 61: 429–444
15 Lambert A, Davies P, Neivandt D. Implementing the theory of sum frequency generation vibrational spectroscopy: a tutorial review. *Appl Spectrosc Rev*, 2005, 40: 103–145
16 Gopalakrishnan S, Liu D, Allen HC, Kuo M, Shultz MJ. Vibrational spectroscopic studies of aqueous interfaces: salts, acids, bases, and nanodrops. *Chem Rev*, 2006, 106: 1155–1175
17 Wang HF, Gan W, Lu R, Rao Y, Wu BH. Quantitative spectral and orientational analysis in surface sum frequency generation vibrational spectroscopy (SFG-VS). *Int Rev Phys Chem*, 2005, 24: 191–256
18 Ye SJ, Nguyen KT, Chen Z. Interactions of alamethicin with model cell membranes investigated using sum frequency generation vibrational spectroscopy in real time *in situ*. *J Phys Chem B*, 2010, 114: 3334–3340
19 Guyotsionnest P, Hunt JH, Shen YR. Sum-frequency vibrational spectroscopy of a Langmuir film: study of molecular-orientation of a two dimensional system. *Phys Rev Lett*, 1987, 59: 1597–1600
20 Zhu XD, Suhr H, Shen YR. Surface vibrational spectroscopy by infrared-visible sum frequency generation. *Phys Rev B*, 1987, 35: 3047–3050
21 Liu W, Wang ZG, Fu L, Leblanc RM, Yan ECY. Lipid compositions modulate fluidity and stability of bilayers: characterization by surface pressure and sum frequency generation spectroscopy. *Langmuir*, 2013, 29: 15022–15031
22 Ma G, Allen HC. DPPC Langmuir monolayer at the air/water interface: probing the tail and head groups by vibrational sum frequency generation spectroscopy. *Langmuir*, 2006, 22: 5341–5349
23 Walker RA, Gruetzmacher JA, Richmond GL. Phosphatidylcholine monolayer structure at a liquid/liquid interface. *J Am Chem Soc*, 1998, 120: 6991–7003
24 Kim J, Kim G, Cremer PS. Investigations of water structure at the solid/liquid interface in the presence of supported lipid bilayers by vibrational sum frequency spectroscopy. *Langmuir*, 2001, 17: 7255–7260
25 Roke S, Schins J, Muller M, Bonn M. Vibrational spectroscopic investigation of the phase diagram of a biomimetic lipid monolayer. *Phys Rev Lett*, 2003, 90: 128101
26 Liu J, Conboy JC. Phase transition of a single lipid bilayer measured by sum-frequency vibrational spectroscopy. *J Am Chem Soc*, 2004, 126: 8894–8895
27 Nickolov ZS, Britt DW, Miller JD. Sum-frequency spectroscopy analysis of two-component Langmuir monolayers and the associated interfacial water structure. *J Phy Chem B*, 2006, 110: 15506–15513
28 Anderson NA, Richter LJ, Stephenson JC, Briggman KA. Characterization and control of lipid layer fluidity in hybrid bilayer membranes. *J Am Chem Soc*, 2007, 129: 2094–2100
29 Ohe C, Goto Y, Noi M, Arai M, Kamijo H, Itoh K. Sum frequency generation spectroscopic studies on phase transitions of phospholipid monolayers containing poly(ethylene oxide) lipids at the air/water interface. *J Phys Chem B*, 2007, 111: 1693–1700
30 Kett PJN, Casford MTL, Davies PB. Sum frequency generation (SFG) vibrational spectroscopy of planar phosphatidylethanolamine hybrid bilayer membranes under water. *Langmuir*, 2010, 26: 9710–9719
31 Liljeblad JFD, Bulone V, Tyrode E, Rutland MW, Johnson CM. Phospholipid monolayers probed by vibrational sum frequency spectroscopy: instability of unsaturated phospholipids. *Biophy J*, 2010, 98: L50–L52
32 Sung W, Seok S, Kim D, Tian CS, Shen YR. Sum-frequency spectroscopic study of Langmuir monolayers of lipids having oppositely charged headgroups. *Langmuir*, 2010, 26: 18266–18272
33 Strader ML, De Aguiar HB, De Beer AGF, Roke S. Label-free spectroscopic detection of vesicles in water using vibrational sum frequency scattering. *Soft Matter*, 2011, 7: 4959–4963
34 Palyvoda O, Bordenyuk AN, Yatawara AK, McCullen E, Chen CC, Benderskii AV, Auner GW. Molecular organization in SAMs used for neuronal cell growth. *Langmuir*, 2008, 24: 4097–4106
35 Diesner MO, Howell C, Kurz V, Verreault D, Koelsch P. *In vitro* characterization of surface properties through living cells. *J Phys Chem Lett*, 2010, 1: 2339–2342
36 Diesner MO, Welle A, Kazanci M, Kaiser P, Spatz J, Koelsch P. *In vitro* observation of dynamic ordering processes in the extracellular matrix of living, adherent cells. *Biointerphases*, 2011, 6: 171–179
37 Howell C, Diesner MO, Grunze M, Koelsch P. Probing the extracellular matrix with sumfrequency generation spectroscopy. *Langmuir*, 2008, 24: 13819–13821
38 Kim SH, Lee CM, Kafle K. Characterization of crystalline cellulose in biomass: basic principles, applications, and limitations of XRD, NMR, IR, Raman, and SFG. *Korean J Chem Eng*, 2013, 30: 2127–2141
39 Barnette AL, Bradley LC, Veres BD, Schreiner EP, Park YB, Park J, Park S, Kim SJ. Selective detection of crystalline cellulose in plant cell walls with sum frequency generation (SFG) vibration spectroscopy. *Biomacromolecules*, 2011, 12: 2434–2439
40 Kong LY, Lee C, Kim SH, Ziegler GR. Characterization of starch polymorphic structures using vibrational sum frequency generation spectroscopy. *J Phys Chem B*, 2014, 118: 1775–1783
41 Kett PJN, Casford MTL, Davies PB. Sum frequency generation vi-

brational spectroscopy of cholesterol in hybrid bilayer membranes. *J Phys Chem B*, 2013, 117: 6455–6465
42 Liu J, Brown KL, Conboy JC. The effect of cholesterol on the intrinsic rate of lipid flip-flop as measured by sum-frequency vibrational spectroscopy. *Faraday Discuss*, 2013, 161: 45–61
43 Ohe C, Sasaki T, Noi M, Goto Y, Itoh K. Sum frequency generation spectroscopic study of the condensation effect of cholesterol on a lipid monolayer. *Anal Bioanal Chem*, 2007, 388: 73–79
44 Bonn M, Roke S, Berg O, Juurlink LBF, Stamouli A, Muller M. A molecular view of cholesterol-induced condensation in a lipid monolayer. *J Phys Chem B*, 2004, 108: 19083–19085
45 Levy D, Briggman KA. Cholesterol/phospholipid interactions in hybrid bilayer membranes. *Langmuir*, 2007, 23: 7155–7161
46 Paszti Z, Keszthelyi T, Hakkel O, Guczi L. Adsorption of amino acids on hydrophilic surfaces. *J Phys Condens Matter*, 2008, 20: 224014
47 Ji N, Shen YR. Optically active sum frequency generation from molecules with a chiral center: amino acids as model systems. *J Am Chem Soc*, 2004, 126: 15008–15009
48 Holinga GJ, York RL, Onorato RM, Thompson CM, Webb NE, Yoon AP, Somorjai GA. An SFG study of interfacial amino acids at the hydrophilic SiO_2 and hydrophobic deuterated polystyrene surfaces. *J Am Chem Soc*, 2011, 133: 6243–6253
49 Ding B, Chen Z. Molecular interactions between cell penetrating peptide pep-1 and model cell membranes. *J Phys Chem B*, 2012, 116: 2545–2552
50 Volkov V, Bonn M. Structural properties of gp41 fusion peptide at a model membrane interface. *J Phys Chem B*, 2013, 117: 15527–15535
51 Roy S, Covert PA, FitzGerald WR, Hore DK. Biomolecular structure at solid/liquid interfaces as revealed by nonlinear optical spectroscopy. *Chem Rev*, 2014, 114: 8388–8415
52 Ye SJ, Wei F, Li HC, Tian KZ, Luo Y. Structure and orientation of interfacial proteins determined by sum frequency generation vibrational spectroscopy: method and application. *Adv Protein Chem Struct Bio*, 2013, 93: 213–255
53 Liu Y, Jasensky J, Chen Z. Molecular interactions of proteins and peptides at interfaces studied by sum frequency generation vibrational spectroscopy. *Langmuir*, 2012, 28: 2113–2121
54 Fu L, Wang ZG, Yan ECY. Chiral vibrational structures of proteins at interfaces probed by sum frequency generation spectroscopy. *Int J Mol Sci*, 2011, 12: 9404–9425
55 Ye SJ, Nguyen KT, Le Clair SV, Chen Z. *In situ* molecular level studies on membrane related peptides and proteins in real time using sum frequency generation vibrational spectroscopy. *J Struct Biol*, 2009, 168: 61–77
56 Keszthelyi T, Hill K, Kiss E. Interaction of phospholipid Langmuir monolayers with an antibiotic peptide conjugate. *J Phys Chem B*, 2013, 117: 6969–6979
57 Niaura G, Kuprionis Z, Ignatjev I, Kazemekaite M, Valincius G, Talaikyte Z, Razumas V, Svendsen A. Probing of lipase activity at air/water interface by sum-frequency generation spectroscopy. *J Phys Chem B*, 2008, 112: 4094–4101
58 Tong YJ, Li N, Liu HJ, Ge AM, Osawa M, Ye S. Mechanistic studies by sum-frequency generation spectroscopy: hydrolysis of a supported phospholipid bilayer by phospholipase A2. *Angew Chem Inter Ed*, 2010, 49: 2319–2323
59 Sartenaer Y, Tourillon G, Dreesen L, Lis D, Mani AA, Thiry PA, Peremans A. Sum-frequency generation spectroscopy of DNA monolayers. *Biosens Bioelectron*, 2007, 22: 2179–2183
60 Howell C, Schmidt R, Kurz V, Koelsch P. Sum-frequency-generation spectroscopy of DNA films in air and aqueous environments. *Biointerphases*, 2008, 3: FC47–FC51
61 Bulard E, Fontaine-Aupart MP, Dubost H, Zheng WQ, Bellon-Fontaine MN, Herry JM, Bourguignon B. Competition of bovine serum albumin adsorption and bacterial adhesion onto surface-grafted ODT: *in situ* study by vibrational SFG and fluorescence confocal microscopy. *Langmuir*, 2012, 28: 17001–17010
62 Apte JS, Gamble LJ, Castner DG, Campbell CT. Kinetics of leucine-lysine peptide adsorption and desorption at $-CH_3$ and –COOH terminated alkylthiolate monolayers. *Biointerphases*, 2010, 5: 97–104
63 Leung BO, Yang Z, Wu SSH, Chou KC. Role of interfacial water on protein adsorption at cross-linked polyethylene oxide interfaces. *Langmuir*, 2012, 28: 5724–5728
64 Han XF, Uzarski JR, Mello CM, Chen Z. Different interfacial behaviors of N- and C-terminus cysteine- modified cecropin P1 chemically immobilized onto polymer surface. *Langmuir*, 2013, 29: 11705–11712
65 Ye SJ, Nguyen KT, Boughton A, Mello C, Chen Z. Orientation difference of chemically immobilized and physically adsorbed biological molecules on polymers detected at the solid/liquid interfaces *in situ*. *Langmuir*, 2010, 26: 6471–6477
66 Baio JE, Weidner T, Ramey D, Pruzinsky L, Castner DG. Probing the orientation of electrostatically immobilized cytochrome C by time of flight secondary ion mass spectrometry and sum frequency generation spectroscopy. *Biointerphases*, 2013, 8: 18
67 Dreesen L, Sartenaer Y, Humbert C, Mani AA, Methivier C, Pradier CM, Thiry PA, Peremans A. Probing ligand-protein recognition with sum-frequency generation spectroscopy: the avidin-biocytin case. *ChemPhysChem*, 2004, 5: 1719–1725
68 Ye SJ, Li HC, Wei F, Jasensky J, Boughton AP, Yang P, Chen Z. Observing a model ion channel gating action in model cell membranes in real time *in situ*: membrane potential change induced alamethicin orientation change. *J Am Chem Soc*, 2012, 134: 6237–6243
69 Scheu R, Chen YX, De Aguiar HB, Rankin BM, Ben-Amotz D, Roke S. Specific ion effects in amphiphile hydration and interface stabilization. *J Am Chem Soc*, 2014, 136: 2040–2047
70 Chen X, Yang TL, Kataoka S, Cremer PS. Specific ion effects on interfacial water structure near macromolecules. *J Am Chem Soc*, 2007, 129: 12272–12279
71 Wei F, Ye SJ, Li HC, Luo Y. Phosphate ions promoting association between peptide and modeling cell membrane revealed by sum frequency generation vibrational spectroscopy. *J Phys Chem C*, 2013, 117: 11095–11103
72 Wei F, Li HC, Ye SJ. Specific ion interaction dominates over hydrophobic matching effects in peptide-lipid bilayer interactions: the case of short peptide. *J Phys Chem C*, 2013, 117: 26190–26196
73 Uehara TM, Marangoni VS, Pasquale N, Miranda PB, Lee KB, Zucolotto V. A detailed investigation on the interactions between magnetic nanoparticles and cell membrane models. *ACS Appl Mater Interfaces*, 2013, 5: 13063–13068
74 Liu J, Conboy JC. 1,2-Diacyl-phosphatidylcholine flip-flop measured directly by sum-frequency vibrational spectroscopy. *Biophy J*, 2005, 89: 2522–2532
75 Boughton AP, Chen Z. Sum frequency generation vibrational spectroscopy: a sensitive technique for the study of biological molecules at interfaces. In: Smentkowski VA. *Surface Analysis and Techniques in Biology*. Berlin: Spriger Verlag, 2014
76 Zhang C, Myers JN, Chen Z. Elucidation of molecular structures at buried polymer interfaces and biological interfaces using sum frequency generation vibrational spectroscopy. *Soft Matter*, 2013, 9: 4738–4761
77 Sung W, Kim D, Shen YR. Sum-frequency vibrational spectroscopic studies of Langmuir monolayers. *Curr Appl Phys*, 2013, 13: 619–632
78 Kim SH, Lee CM, Kafle K. Structure and orientation of interfacial proteins determined by sum frequency generation vibrational spectroscopy: method and application. *Korean J Chem Eng*, 2013, 30: 2127–2141
79 Zhang XX, Han XF, Wu FG, Jasensky J, Chen Z. Nano-bio interfaces probed by advanced optical spectroscopy: from model system studies to optical biosensors. *Chin Sci Bull*, 2013, 58: 2537–2556

80 Chen Z. Molecular structures of buried polymer interfaces and biological interfaces detected by sum frequency generation vibrational spectroscopy. *Acta Phys Chim Sin*, 2012, 28: 504–521
81 Roke S. Nonlinear spectroscopy of biointerface. *Int J Mat Res*, 2011, 102: 906–912
82 Roke S. Nonlinear optical spectroscopy of soft matter interfaces. *ChemPhysChem*, 2009, 10: 1380–1388
83 Bonn M, Campen RK. Optical methods for the study of dynamics in biological membrane models. *Surf Sci*, 2009, 603: 1945–1952
84 Le Clair SV, Nguyen K, Chen Z. Sum frequency generation studies on bioadhesion: elucidating the molecular structure of proteins at interfaces. *J Adhesion*, 2009, 85: 484–511
85 Ma G, Allen HC. New insights into lung surfactant monolayers using vibrational sum frequency generation spectroscopy. *Photochem Photobio*, 2006, 82: 1517–1529
86 Chen XY, Chen Z. SFG studies on interactions between antimicrobial peptides and supported lipid bilayers. *Biochim Biophys Acta*, 2006, 1758: 1257–1273
87 Chen XY, Clarke ML, Wang J, Chen Z. Sum frequency generation vibrational spectroscopy studies on molecular conformation and orientation of biological molecules at interfaces. *Int J Mod Phys B*, 2005, 19: 691–713
88 Vogel V. What do nonlinear optical techniques have to offer the biosciences? *Curr Opinn Colloid Interface Sci*, 1996, 1: 257–263
89 Kneipp K, Kneipp H, Itzkan I, Dasari RR, Feld MS. Ultrasensitive chemical analysis by Raman spectroscopy. *Chem Rev*, 1999, 99: 2957–2975
90 Brown TL. Infrared intensities and molecular structure. *Chem Rev*, 1958, 58: 581–609
91 Stuart BH. *Infrared Spectroscopy: Fundamentals and Applications.* UK: John Wiley, 2004
92 Johnson CM, Tyrode E, Baldelli S, Rutland MW, Leygraf C. A vibrational sum frequency spectroscopy study of the liquid/gas interface of acetic acid-water mixtures: 1. Surface speciation. *J Phys Chem B*, 2005, 109: 321–328
93 Tyrode E, Johnson CM, Rutland MW, Day JPR, Bain CD. A study of the adsorption of ammonium perfluorononanoate at the air/liquid interface by vibrational sum-frequency spectroscopy. *J Phys Chem C*, 2007, 111: 316–329
94 Johnson CM, Tyrode E. Study of the adsorption of sodium dodecyl sulfate (SDS) at the air/water interface: targeting the sulfate headgroup using vibrational sum frequency spectroscopy. *Phys Chem Chem Phys*, 2005, 7: 2635–2640
95 Hore DK, Beaman DK, Richmond GL. Surfactant headgroup orientation at the air/water interface. *J Am Chem Soc*, 2005, 127: 9356–9357
96 Hore DK, Beaman DK, Parks DH, Richmond GL. Whole-molecule approach for determining orientation at isotropic surfaces by nonlinear vibrational spectroscopy. *J Phys Chem B*, 2005, 109: 16846–16851
97 Wei F, Ye SJ. Molecular-level insights into N–N π-bond rotation in the pH-induced interfacial isomerization of 5-octadecyloxy-2-(2-pyridylazo)phenol monolayer investigated by sum frequency generation vibrational spectroscopy. *J Phys Chem C*, 2012, 116: 16553–16560
98 Ye SJ, Wei F. An approach to compatible multiple nonlinear vibrational spectroscopy measurements using commercial sum frequency generation system. *Analyst*, 2011, 136: 2489–2494
99 Sugiharto AB, Johnson CM, De Aguiar HB, Alloatti L, Roke S. Generation and application of high power femtosecond pulses in the vibrational fingerprint region. *Appl Phys B*, 2008, 91: 315–318
100 Sugiharto AB, Johnson CM, Dunlop IE, Roke S. Delocalized surface modes reveal three-dimensional structures of complex biomolecules. *J Phys Chem C*, 2008, 112: 7531–7534
101 Barth A, Zscherp C. What vibrations tell about proteins. *Quar Rev Biophys*, 2002, 35: 369–430
102 Tamm L, Tatulian SA. Infrared spectroscopy of proteins and peptides in lipid bilayers. *Quar Rev Biophys*, 1997, 30: 365–429
103 Oladepo SA, Xiong K, Hong ZM, Asher SA, Hander J, Lednev IK. UV resonance Raman investigations of peptide and protein structure and dynamics. *Chem Rev*, 2012, 112: 2604–2628
104 Belkin MA, Shen YR. Non-linear optical spectroscopy as a novel probe for molecular chirality. *Inter Rev Phy Chem*, 2005, 24: 257–299
105 Haupert LM, Simpson GJ. Chirality in nonlinear optics. *Annu Rev Phys Chem*, 2009, 60: 345–365
106 Belkin MA, Han SH, Wei X, Shen YR. Sum-frequency generation in chiral liquids near electronic resonance. *Phys Rev Lett*, 2001, 87: 113001
107 Belkin MA, Kulakov TA, Ernst KH, Yan L, Shen YR. Sum-frequency vibrational spectroscopy on chiral liquids: a novel technique to probe molecular chirality. *Phys Rev Lett*, 2000, 85: 4474–4476
108 Ji N, Ostroverkhov V, Belkin M, Shiu YJ, Shen YR. Toward chiral sum-frequency spectroscopy. *J Am Chem Soc*, 2006, 128: 8845–8848
109 Ji N, Shen YR. A dynamic coupling model for sum frequency chiral response from liquids composed of molecules with a chiral side chain and an achiral chromophore. *J Am Chem Soc*, 2005, 127: 12933–12942
110 Belkin MA, Shen YR. Doubly resonant IR-UV sum-frequency vibrational spectroscopy on molecular chirality. *Phys Rev Lett*, 2003, 91: 213907
111 Mitchell SA, McAloney RA. Second harmonic optical activity of tryptophan derivatives adsorbed at the air/water interface. *J Phys Chem B*, 2004, 108: 1020–1029
112 Reiser KM, McCourt AB, Yankelevich DR, Knoesen A. Structural origins of chiral second-order optical nonlinearity in collagen: amide I band. *Biophys J*, 2012, 103: 2177–2186
113 Wang ZG, Fu L, Yan ECY. C–H stretch for probing kinetics of self-assembly into macromolecular chiral structures at interfaces by chiral sum frequency generation spectroscopy. *Langmuir*, 2013, 29: 4077–4083
114 Xiao DQ, Fu L, Liu J, Batista VS, Yan ECY. Amphiphilic adsorption of human islet amyloid polypeptide aggregates to lipid/aqueous interfaces. *J Mol Biol*, 2012, 421: 537–547
115 Conboy JC, Kriech MA. Measuring melittin binding to planar supported lipid bilayer by chiral second harmonic generation. *Anal Chimica Acta*, 2003, 496: 143–153
116 Rocha-Mendoza I, Yankelevich DR, Wang M, Reiser KM, Frank CW, Knoesen A. Sum frequency vibrational spectroscopy: the molecular origins of the optical second-order nonlinearity of collagen. *Biophys J*, 2007, 93: 4433–4444
117 Wang J, Chen XY, Clarke ML, Chen Z. Detection of chiral sum frequency generation vibrational spectra of proteins and peptides at interfaces *in situ*. *Proc Natl Acad Sci USA*, 2005, 102: 4978–4983
118 Nguyen KT, King JT, Chen Z. Orientation determination of interfacial β-sheet structures *in situ*. *J Phys Chem B*, 2010, 114: 8291–8300
119 Fu L, Liu J, Yan ECY. Chiral sum frequency generation spectroscopy for characterizing protein secondary structures at interfaces. *J Am Chem Soc*, 2011, 133: 8094–8097
120 Fu L; Ma G, Yan ECY. *In situ* misfolding of human islet amyloid polypeptide at interfaces probed by vibrational sum frequency generation. *J Am Chem Soc*, 2010, 132: 5405–5412
121 Fu L, Xiao DQ, Wang ZG, Batista VS, Yan ECY. Chiral sum frequency generation for in situ probing proton exchange in antiparallel β-sheets at interfaces. *J Am Chem Soc*, 2013, 135: 3592–3598
122 Ma SL, Li HC, Tian KZ, Ye SJ, Luo Y. *In situ* and real time SFG measurements reveal organization and transport of cholesterol analog 6-ketocholestanol in cell membrane. *J Phys Chem Lett*, 2014, 5:

419–424
123 Stokes GY, Gibbs-Davis JM, Boman FC, Stepp BR, Condie AG, Nguyen ST, Geiger FM. Making "sense" of DNA. *J Am Chem Soc*, 2007, 129: 7492–7493
124 Walter SR, Geiger FM. DNA on stage: showcasing oligonucleotides at surfaces and interfaces with second harmonic and vibrational sum frequency generation. *J Phys Chem Lett*, 2009, 1: 9–15
125 Li HC, Ye SJ, Wei F, Ma SL, Luo Y. *In situ* molecular-level insights into the interfacial structure changes of membrane-associated prion protein fragment [118–135] investigated by sum frequency generation vibrational spectroscopy. *Langmuir*, 2012, 28: 16979–16988
126 Lingwood D, Simons K. Lipid rafts as a membrane-organizing principle. *Science*, 2010, 327: 46–50
127 Barnes WL, Dereux A, Ebbesen TW. Surface plasmon subwavelength optics. *Nature*, 2003, 424: 824–830
128 Maier SA. *Plasmonics: Fundamentals and Applications*. New York: Springer, 2007
129 Lis D, Caudano Y, Henry M, Demoustier-Champagne S, Ferain E, Cecchet F. Selective plasmonic platforms based on nanopillars to enhance vibrational sum-frequency generation spectroscopy. *Adv Optical Mater*, 2013, 1: 244–255
130 Willets KA, Van Duyne RP. Localized surface plasmon resonance spectroscopy and sensing. *Annu Rev Phys Chem*, 2007, 58: 267–297
131 Stiles PL, Dieringer JA, Shah NC, Van Duyne RR. Surface-enhanced Raman spectroscopy. *Annu Rev Anal Chem*, 2008, 1: 601–626
132 Alieva EV, Kuzik LA, Yakovlev VA, Knippels G, van der Meer AFG, Mattei G. Spectroscopy of a thin fullerene film on silver using sum frequency generation enhanced by visible surface plasmon-polaritons. *Chem Phys Lett*, 1999, 302: 528–532
133 Alieva EV, Kuzik LA, Yakovlev VA. Sum frequency generation spectroscopy of thin organic films on silver using visible surface plasmon generation. *Chem Phys Lett*, 1998, 292: 542–546
134 Baldelli S, Eppler AS, Anderson E, Shen YR, Somorjai GA. Surface enhanced sum frequency generation of carbon monoxide adsorbed on platinum nanoparticle arrays. *J Chem Phys*, 2000, 113: 5432–5438
135 Li QF, Kuo CW, Yang Z, Chen PL, Chou KC. Surface-enhanced IR-visible sum frequency generation vibrational spectroscopy. *Phys Chem Chem Phys*, 2009, 11: 3436–3442
136 Pluchery O, Humbert C, Valamanesh M, Lacaze E, Busson B. Enhanced detection of thiophenol adsorbed on gold nanoparticles by SFG and DFG nonlinear optical spectroscopy. *Phys Chem Chem Phys*, 2009, 11: 7729–7737
137 Liu WT, Shen YR. *In situ* sum-frequency vibrational spectroscopy of electrochemical interfaces with surface plasmon resonance. *Proc Natl Acad Sci USA*, 2014, 111: 1293–1297
138 Jang JH, Jacob J, Santos G, Lee TR, Baldelli S. Image contrast in sum frequency generation microscopy based on monolayer order and coverage. *J Phys Chem C*, 2013, 117: 15192–15202
139 Chung CY, Boik J, Potma EO. Biomolecular imaging with coherent nonlinear vibrational microscopy. *Annu Rev Phys Chem*, 2013, 64: 77–99
140 Raghunathan V, Han Y, Korth O, Ge NH, Potma EO. Rapid vibrational imaging with sum frequency generation microscopy. *Opt Lett*, 2011, 36: 3891–3893
141 Sakai M, Kikuchi K, Fujii M. Quaternary and secondary structural imaging of a human hair by a VSFG-detected IR super-resolution microscope. *Chem Phys*, 2013, 419: 261–265
142 Smith KA, Conboy JC. A simplified sum-frequency vibrational imaging setup used for imaging lipid bilayer arrays. *Anal Chem*, 2012, 84: 8122–8126
143 Inoue K, Fujii M, Sakai M. Development of a non-scanning vibrational sum-frequency generation detected infrared super-resolution microscope and its application to biological cells. *Appl Spectrosc*, 2010, 64: 275–281
144 Ji N, Zhang K, Yang H, Shen YR. Three-dimensional chiral imaging by sum-frequency generation. *J Am Chem Soc*, 2006, 128: 3482–3483
145 Kubota J, Domen K. Study of the dynamics of surface molecules by time-resolved sum-frequency generation spectroscopy. *Anal Bioanal Chem*, 2007, 388: 17–27
146 Smits M, Ghosh A, Bredenbeck J, Yamamoto S, Muller M, Bonn M. Ultrafast energy flow in model biological membranes. *New J Phys*, 2007, 9: 390
147 Arnolds H, Bonn M. Ultrafast surface vibrational dynamics. *Surf Sci Rep*, 2010, 65: 45–66
148 Backus EHG, Eichler A, Kleyn AW, Bonn M. Real-time observation of molecular motion on a surface. *Science*, 2005, 310: 1790–1793
149 McGuire JA, Shen YR. Ultrafast vibrational dynamics at water interfaces. *Science*, 2006, 313: 1945–1948
150 Bredenbeck J, Ghosh A, Nienhuys HK, Bonn M. Interface-specific ultrafast two-dimensional vibrational spectroscopy. *Acc Chem Res*, 2009, 42: 1332–1342
151 Eftekhari-Bafrooei A, Borguet E. Effect of hydrogen-bond strength on the vibrational relaxation of interfacial water. *J Am Chem Soc*, 2010, 132: 3756–3761
152 Rao Y, Xu M, Jockusch S, Turro NJ, Eisenthal KB. Dynamics of excited state electron transfer at a liquid interface using time-resolved sum frequency generation. *Chem Phys Lett*, 2012, 544: 1–6
153 Nihonyanagi S, Mondal JA, Yamaguchi S, Tahara T. Structure and dynamics of interfacial water studied by heterodyne-detected vibrational sum-frequency generation. *Annu Rev Phys Chem*, 2013, 64: 579–603